Cement & Concrete Composites 30 (2008) 822–830

Contents lists available at ScienceDirect

Cement & Concrete Composites

journal homepage: www.elsevier.com/locate/cemconcomp

Post-repair performance of eccentrically loaded RC columns wrapped with CFRP composites

Tamer El Maaddawy *

UAE-University, Al-Ain, Abu Dhabi, P.O. Box 17555, United Arab Emirates

ARTICLE INFO

Article history:
Received 3 September 2007
Received in revised form 18 June 2008
Accepted 19 June 2008
Available online 27 June 2008

Keywords:
Concrete
Columns
Corrosion
CFRP
Eccentric
Repair

ABSTRACT

This paper presents the results of a research program for examining the post-repair performance of eccentrically loaded corrosion-damaged reinforced concrete (RC) columns wrapped with carbon fiber reinforced polymer (CFRP) composites. The specimens, except a control undamaged group, were initially exposed to accelerated corrosion for 30 days using an impressed current technique. Following the initial corrosion, the damaged specimens were either repaired with full or partial CFRP wrapping systems or kept unrepaired. A group from the damaged specimens were further exposed to 60 days of corrosion exposure. All specimens were tested to failure under various eccentric loading with a nominal eccentricity-to-section height ratio (e/h) in the range of 0.3–0.86. Test results showed that full CFRP wrapping system effectively reduced the post-repair corrosion rate relative to that of the unwrapped specimens whereas partial CFRP wrapping had almost no effect on the steel mass loss. The strengths of the damaged specimens fully wrapped with CFRP were higher than those of the control specimens at the end of the post-repair corrosion phase. The strengths of the damaged partially wrapped specimens were higher than those of the control at nominal e/h values $\leqslant 0.43$. At higher e/h values, the strengths of the partially wrapped specimens were lower than those of the control but still higher than those of the damaged unrepaired specimens. An analytical model that accounts for the confinement effect of the CFRP and the change in geometry under eccentric loading was employed to predict the columns' strength. The model's predictions were validated against test results.

1. Introduction

Chloride-induced corrosion in reinforced concrete (RC) structures is a major worldwide durability problem. Reinforced concrete structures located in industrial regions are also vulnerable to carbonation-induced corrosion due to the increased concentration of carbon dioxide. The appearance of the first surface corrosion crack is usually used to define the end of the functional service life of the structure where structural rehabilitation is required [1–3].

Externally bonded carbon fiber reinforced polymers (CFRP) composite system has emerged as an effective innovative solution for rehabilitation of corrosion-damaged RC beams [4–6] and axially loaded columns [7–9]. CFRP wrapping system was found less effective in increasing the structural capacity of undamaged RC columns under combined flexural and axial loading [10–12]. Although RC columns are often exposed to eccentric loading, the effectiveness of CFRP wrapping system to upgrade corrosion-damaged eccentrically loaded RC columns has received little attention in the literature.

The present work is the second phase (phase II) of a research program aimed at examining the viability of CFRP wrapping system to upgrade corrosion-damaged RC columns in the short-and-long term when tested to failure under eccentric loading. Results of phase I showed that CFRP wrapping system was effective in increasing the structural capacity of eccentrically loaded corroded columns in the short term [13]. In this paper, the post-repair performance of CFRP-repaired columns under additional corrosion exposure is examined. An analytical model proposed by the author for performance prediction of eccentrically loaded RC columns wrapped with CFRP [14] was employed to verify test results. The model takes into consideration the change in eccentricity caused by the lateral displacement under eccentric loading and the confinement effect caused by CFRP. The effect of corrosion damage was accounted for in the analysis of the present study. The analytical and experimental results were in good agreement.

2. Experimental program

2.1. Specimen details

Test specimen was a square RC column (125 × 125 × 500 mm) with end corbels, 250 × 250 × 350 mm each (Fig. 1). Because of

* Tel.: +971 50 8310915; fax: +971 3 7623154.
E-mail address: tamer.maaddawy@uaeu.ac.ae

0958-9465/$ - see front matter © 2008 Elsevier Ltd. All rights reserved.
doi:10.1016/j.cemconcomp.2008.06.009

Notation

e	load eccentricity	P_{exp}	experimental compression strength
e_{ext}	external eccentricity	P_n	nominal compression strength
e_{int}	internal eccentricity	P_{pre}	predicted compression strength
$e_{nominal}$	nominal eccentricity	ε_{cc}	ultimate compressive strain of CFRP-confined concrete under eccentric loading
f'_c	compressive strength of unconfined concrete	ε_{ccu}	ultimate compressive strain of CFRP-confined concrete under concentric loading
f'_{cc}	compressive strength of CFRP-confined concrete under eccentric loading	ε_{cu}	ultimate compressive strain of unconfined concrete
f'_{cco}	compressive strength of CFRP-confined concrete under concentric loading	ϕ	mid-height curvature
f_l	effective lateral confining pressure provided by CFRP	Δ	lateral mid-height displacement
h	depth of the column section	Δ_{exp}	experimental lateral mid-height displacement
M_n	nominal moment strength	Δ_{pre}	predicted lateral mid-height displacement

the limitation in the capacity of the reaction frame available at the structural laboratory of the UAE-University, a larger cross section could not be employed. The longitudinal steel reinforcement in the test region consisted of four No. 10 deformed steel bars with a total area of about 298.5 mm^2. The column's ties in the test region (the middle 500 mm) were 6 mm diameter plain bars having a clear concrete cover of 15 mm. A tubing stainless steel bar with an outer diameter of 8 mm and a wall thickness of 1 mm was placed in the middle of the column to act as a cathode during the accelerated corrosion process. To facilitate electrical connections for the accelerated corrosion, the longitudinal steel and the stainless steel tube were extended about 100 mm out of one end of the specimen.

2.2. Materials properties

Normal strength concrete with mix proportions by weight (cement:sand:gravel:w/c = 1:2.6:2.4:0.65) was used in the present study. Three concrete cylinders, each having a diameter of 150 mm and a length of 300 mm, were cast from the same mix used in fabrication of test specimens to determine the concrete compression strength. The concrete compression strength was on average 28.5 MPa with a corresponding standard deviation of 2.5 MPa. To simulate chloride contamination of concrete, 3% NaCl by weight of cement was added to the concrete mixture used to cast the middle 400 mm of the column. The longitudinal steel reinforcement was Grade 520. Three steel samples were tested under

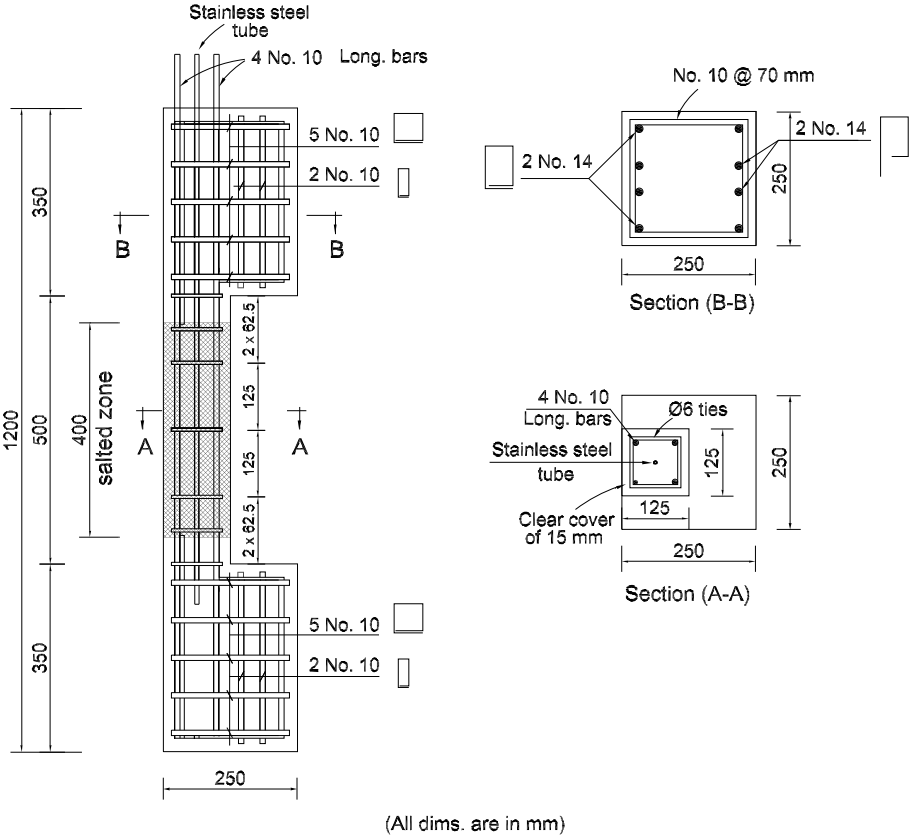

Fig. 1. Details of test specimen [13].

uniaxial tension to determine the tensile strength. The measured yield and ultimate strengths of the longitudinal steel were on average 550 and 725 MPa, respectively. The CFRP composite used in the present study was unidirectional and consisted of *SikaWrap Hex 230C* fibers and *Sikadur Hex 300* resin. For a cured CFRP composite sheet the manufacturer's data sheet specifies a typical modulus of elasticity of 65.4 GPa, an ultimate tensile strain of 1.33%, and a thickness of 0.381 mm.

2.3. Test matrix

As shown in Table 1, the research project is designed to be implemented in two phases. Specimens of phase I [13] were divided into four main groups, [A], [B], [C], and [D] whereas specimens of phase II (current phase) consisted of three groups, [E], [F], and [G]. All specimens, except those of group [A], were initially exposed to 30 days of accelerated corrosion exposure. Following the initial corrosion, specimens of group [B] were tested to failure without repair while specimens of groups [C] and [D] were repaired with full and partial CFRP wrapping systems, respectively, then tested to failure under various eccentric loading. A schematic for the full and partial CFRP wrapping schemes used to repair the corrosion-damaged specimens are shown in Fig. 2 [13]. In both schemes one layer of CFRP sheet was wrapped around the column's section in the test region with the fibers oriented in the transverse direction with an overlap of about 50 mm. The specimens' corners were rounded to a radius of about 10 mm prior to CFRP application. Details of surface preparation and CFRP application are given in Ref. [13]. The full and partial CFRP wrapping schemes corresponded to effective confinement ratios (f_l/f'_c) of about 0.2 and 0.12, respectively [14] where f_l is the effective lateral confining pressure provided by CFRP and f'_c is the compression strength of an unconfined concrete. To examine the post-repair performance, specimens of phase II were further exposed to 60 days of accelerated corrosion. Specimens of groups [F] and [G] were fully and partially wrapped with CFRP, respectively while specimens of group [E] were kept unwrapped during the post-repair corrosion phase. All specimens were eventually tested to failure under various eccentric loading in the range of 0.3–0.86.

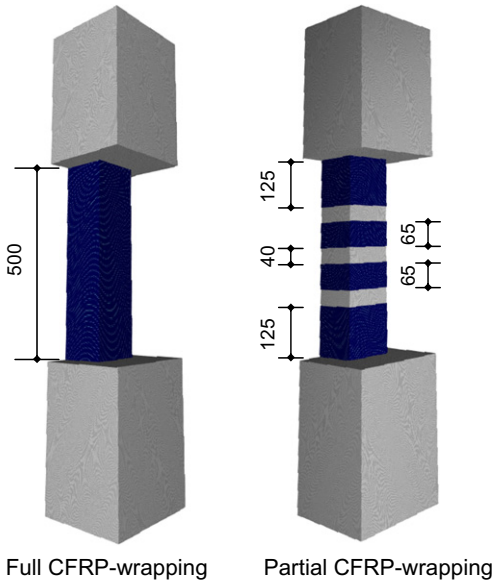

Fig. 2. CFRP repair schemes [13].

2.4. Test set-up and procedure

All corroded specimens were initially subjected to accelerated corrosion for 30 days under a constant impressed current of

Table 1
Test matrix

Phase	Group	Specimen[a]	Initial corrosion time (days)	Additional corrosion time (days)	Confinement condition	Nominal e/h
Phase I [13]	[A]	NUW-e1	–	–	No wrapping	0.30
		NUW-e2	–	–	No wrapping	0.43
		NUW-e3	–	–	No wrapping	0.57
		NUW-e4	–	–	No wrapping	0.86
	[B]	CUW-e1/30	30	–	No wrapping	0.30
		CUW-e2/30	30	–	No wrapping	0.43
		CUW-e3/30	30	–	No wrapping	0.57
		CUW-e4/30	30	–	No wrapping	0.86
	[C]	CFW-e1/30	30	–	Full wrapping	0.30
		CFW-e2/30	30	–	Full wrapping	0.43
		CFW-e3/30	30	–	Full wrapping	0.57
		CFW-e4/30	30	–	Full wrapping	0.86
	[D]	CPW-e1/30	30	–	Partial wrapping	0.30
		CPW-e2/30	30	–	Partial wrapping	0.43
		CPW-e3/30	30	–	Partial wrapping	0.57
		CPW-e4/30	30	–	Partial wrapping	0.86
Phase II	[E]	CUW-e1/90	30	60	No wrapping	0.30
		CUW-e2/90	30	60	No wrapping	0.43
		CUW-e3/90	30	60	No wrapping	0.57
		CUW-e4/90	30	60	No wrapping	0.86
	[F]	CFW-e1/90	30	60	Full wrapping	0.30
		CFW-e2/90	30	60	Full wrapping	0.43
		CFW-e3/90	30	60	Full wrapping	0.57
		CFW-e4/90	30	60	Full wrapping	0.86
	[G]	CPW-e1/90	30	60	Partial wrapping	0.30
		CPW-e2/90	30	60	Partial wrapping	0.43
		CPW-e3/90	30	60	Partial wrapping	0.57
		CPW-e4/90	30	60	Partial wrapping	0.86

[a] N and C refer to no corrosion and corrosion, respectively. UW, FW, and PW refer to unwrapped, fully wrapped, and partially wrapped specimens, respectively. e1, e2, e3, and e4 refer to nominal e/h values of 0.3, 0.43, 0.57, and 0.86, respectively. 30 and 90 refer to total times of corrosion exposure.

Fig. 3. Structural test set-up.

75 mA that corresponded to a current density of about 90 μA/cm^2. The specimens were connected in series in order to ensure that the electrical current passing through all specimens was the same during the initial corrosion exposure. Fogging compressed air mist nozzle was utilized to spray mist over the test specimens to facilitate corrosion reactions.

Specimens of phase II were further exposed to additional 60 days of accelerated corrosion under fixed potentials. In the first 30 days of the additional corrosion exposure the applied fixed potential was 12 V while in the last 30 days the fixed potential was increased to 15 V. The power supply used to impress the current has several outlets through which the same applied potential could be fixed between the ends of each group of phase II during the post-repair corrosion phase. The power supply has an LCD screen that can display the instantaneous current, which allowed continuous monitoring of the fluctuation in the post-repair impressed current with time. The current passing in one of the three groups was monitored by cutting off the current through the other two groups. After current stabilization, the current passing in the connected group was recorded. All groups were subjected to the same procedure before recording the current values.

In the structural test to failure, the load was applied monotonically by means of a hydraulic jack and recorded by means of a load cell. The longitudinal concrete deformation and the lateral mid-height displacement were measured by means of linear variable differential transducers (LVDTs). Fig. 3 shows the structural test set-up.

3. Experimental results

3.1. Summary of the results of phase I

Results of phase I showed that the initial 30 days of corrosion exposure (4.25% measured steel mass loss) corresponded to a maximum corrosion crack width of about 0.4 ± 0.12 mm. Structural test results showed that 4.25% steel mass loss had no noticeable effect on the strength of eccentrically loaded RC columns. At nominal e/h of 0.3, the strength of the damaged column repaired with full CFRP wrapping system was about 40% higher than that of the control. However, the strength gain decreased as e/h was increased. Only 5% enhancement in the column's strength over the control was recorded at nominal e/h of 0.86. At nominal e/h of 0.3, the strength of the damaged column partially wrapped with CFRP was 8% lower than that of its counterpart repaired with full CFRP wrapping but still 28% higher than that of the control undamaged column. At higher e/h values, the confinement level had a negligible effect on the columns' strength. Detailed description and discussion of the results of phase I are presented in Ref. [13].

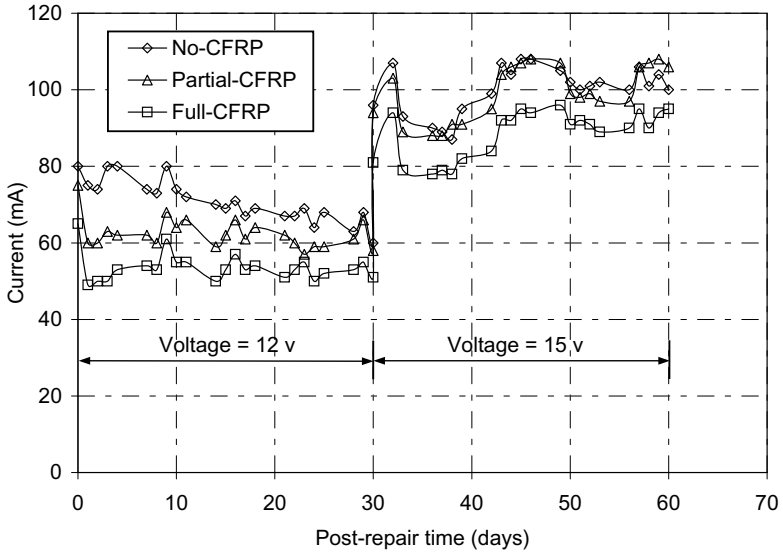

Fig. 4. Monitored current versus post-repair time relationship.

3.2. Results of phase II

3.2.1. Current monitoring

Fig. 4 shows the current measured in each group versus post-repair time relationship. From this figure, it is evident that for the same applied potential, full CFRP wrapping effectively reduced the monitored current. The current reduction was more pronounced at the lower applied potential (12 V). The current measured in the specimens fully wrapped with CFRP was on average about 25% and 12% lower than that measured in the unwrapped specimens at fixed applied potentials of 12 and 15 V, respectively. Full CFRP wrapping may have reduced the diffusion rate of oxygen and moisture into the concrete which increased the apparent resistivity of the specimen, impeded the cathodic reaction at the surface of the embedded stainless steel tube, and thus reduced the corresponding current. From the same figure it can be seen that partial CFRP wrapping was less effective than full wrapping in reducing the current. It resulted in only 12% reduction in the current, compared with that of the unrepaired specimens, at applied fixed potential of 12 V whereas it had no noticeable effect on the measured current at a fixed applied potential of 15 V.

3.2.2. Steel mass loss

Sample corroded steel bars were extracted from some of test specimens after the structural test to failure to measure the steel mass loss caused by corrosion. The corroded steel bars were cleaned of rust using the chemical cleaning procedure, C.3.5, specified by the ASTM Standard G1-90 [15] (Fig. 5). The measured steel mass loss at the end of the first corrosion phase (30 days) was on average about 4.25%. All damaged specimens are assumed to have same initial steel mass loss (4.25%) at the end of the first phase of corrosion exposure. Fig. 6 shows the effect of CFRP wrapping on the post-repair steel mass loss. From this figure it can be seen that full CFRP wrapping resulted in about 28% reduction in the post-repair steel mass loss relative to that of the unwrapped specimens. On the contrary, partial CFRP wrapping had almost no effect on the measured post-repair steel mass loss compared with that of the unwrapped specimens.

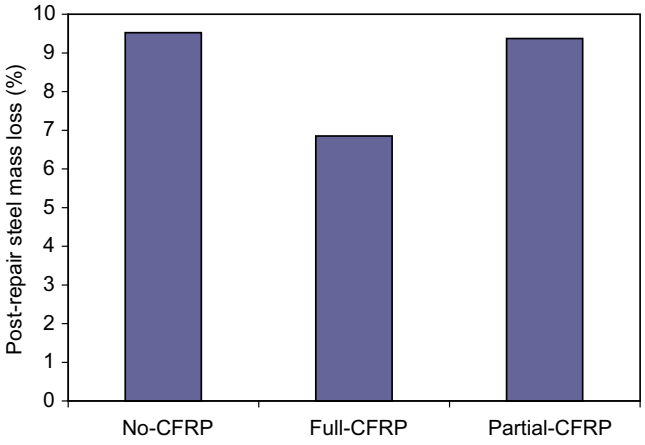

Fig. 6. Effect of CFRP wrapping on measured post-repair steel mass loss.

3.2.3. Corrosion cracking

All corroded specimens exhibited longitudinal corrosion cracking parallel to the longitudinal steel reinforcement. The corrosion crack width at the end of each phase of corrosion was measured by a microscope that provides a magnification of 25× and a resolution of ±0.05 mm. The maximum corrosion crack width measured in the corroded unwrapped specimens at the end of the second phase (13.8% measured steel mass loss) was on average about 1.65 ± 0.35 mm. Fig. 7 shows a typical corrosion crack pattern and width at the end of the second phase of corrosion exposure.

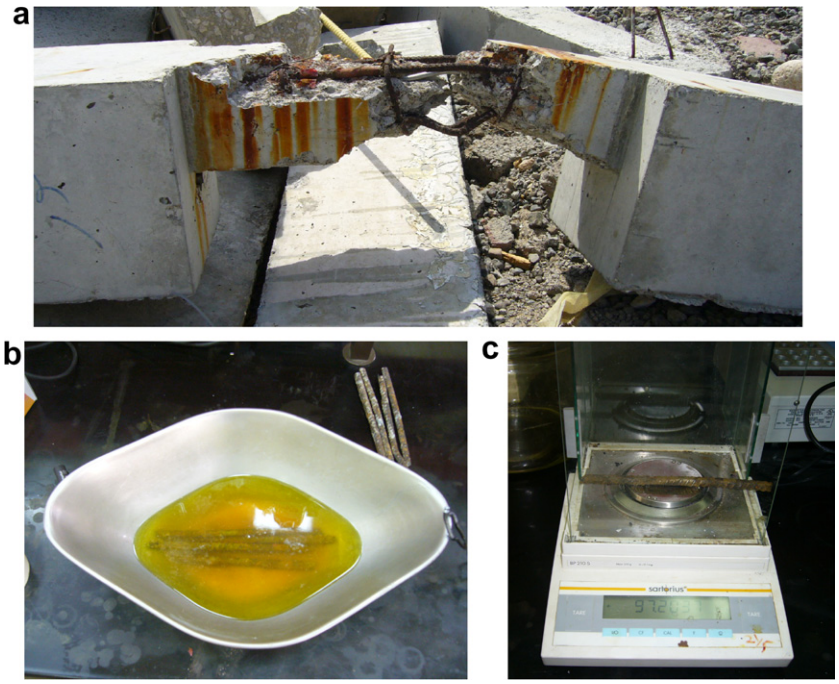

Fig. 5. Steel mass loss measurements: (a) extraction of steel samples, (b) rust removal and (c) steel weighing.

3.2.4. Structural performance

The load versus lateral mid-height displacement curves for specimens of groups [A] and [E] are shown in Fig. 8 while Fig. 9 depicts the load–lateral displacement curves for specimens of groups [F] and [G]. The compression strength and deflection capacity of the specimens are summarized in Table 2.

3.2.4.1. Mode of failure. All specimens of group [A], except NUW-e4, exhibited a brittle mode of failure without warning. Specimen NUW-e4 exhibited a ductile mode of failure where yielding of tension steel preceded crushing of concrete. Specimens CUW-e1/90 and CUW-e2/90 from group [E] exhibited a compression mode of failure whereas specimens CUW-e3/90 and CUW-e4/90 had a tension mode of failure. Because of the severe corrosion damage, the whole concrete cover at compression side was spalled off at the onset of failure for specimens of group [E] (Fig. 10a). All wrapped specimens failed by rupture of the CFRP in transverse direction and bursting of concrete at compression side (Fig. 10b). In specimens CFW-e1/90 and CPW-e1/90, rupture of CFRP occurred without yielding of tension steel. In all other wrapped specimens, rupture of CFRP was preceded by yielding of the tension steel (see Fig. 9).

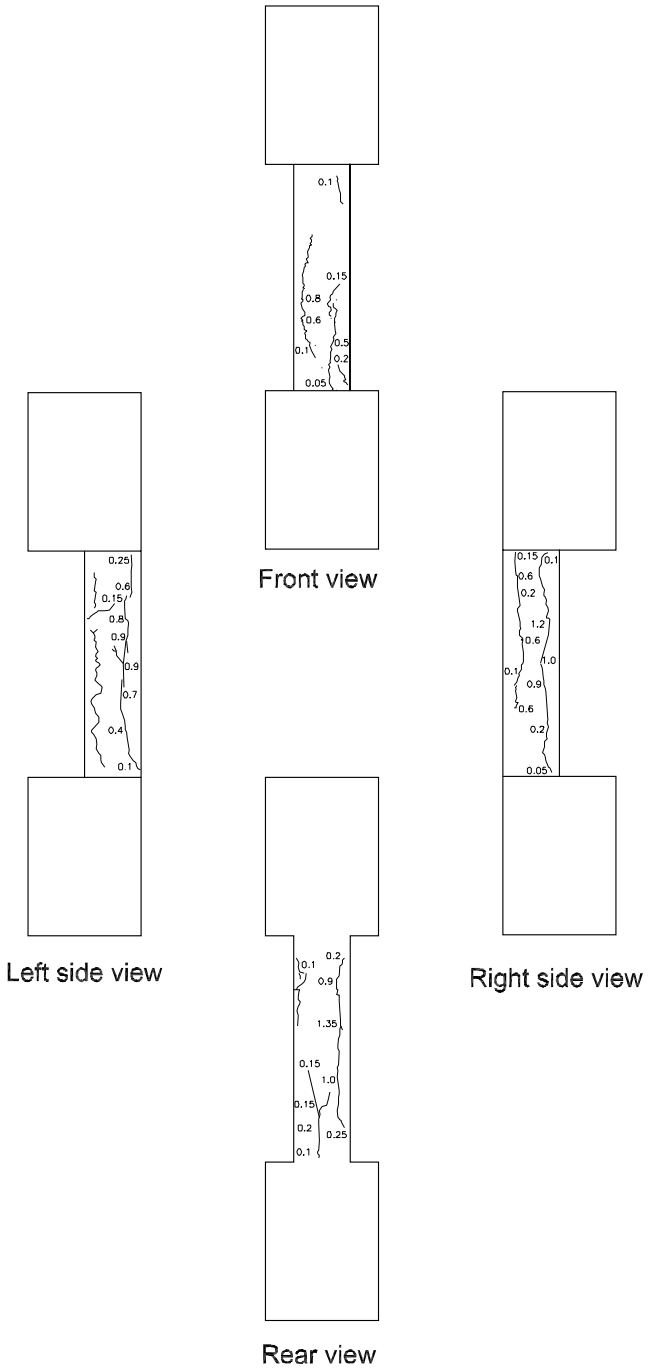

Fig. 7. Typical corrosion crack pattern/width at 13.8% steel mass loss.

3.2.4.2. Strength. From Fig. 8, it is evident that 13.8% corrosion significantly reduced the load carrying capacity of eccentrically loaded RC columns. The reduction in the strength caused by corrosion was in the range of 20–31%. The percent strength reduction was much greater than the percent reduction in the steel mass loss. This is attributable to cracking and deterioration of the concrete cover caused by corrosion which reduced the concrete section size and thus further reduced the strength. From Table 2, it can be seen that despite corrosion damage the strengths of specimens of group [F] fully wrapped with CFRP were still 35%, 24%, 3%, and 1% higher than those of the control undamaged specimens at nominal e/h values of 0.3, 0.43, 0.57, and 0.86, respectively. The strengths of specimens of group [G] partially wrapped with CFRP were 14% and 6% higher than those of the control specimens at e/h values of 0.3 and 0.43, respectively. At higher e/h values the strength was lower than that of the control but still higher than that of the damaged unrepaired specimens.

3.2.4.3. Deflection capacity. For the unwrapped specimens, 13.8% corrosion reduced the deflection capacity when a compression mode of failure was dominated. About 23% average reduction in deflection capacity was recorded at e/h values of 0.3 and 0.43. The deflection capacity of the unwrapped columns was not reduced due to the 13.8% corrosion at e/h values of 0.57 and 0.86. At the end of the post-repair corrosion phase, full CFRP wrapping system resulted in an increase in deflection capacity, relative to that of specimens of group [E] that were corroded but unwrapped with CFRP. About 43% average increase in the deflection capacity due to full CFRP wrapping was recorded at e/h values of 0.3 and 0.43. The increase in the deflection capacity was less pronounced at higher e/h values. About 20% average increase in deflection capacities due to full CFRP wrapping was recorded at e/h values of 0.57 and 0.86. The deflection capacities of the columns partially wrapped with CFRP were almost the same as those of their counterparts repaired with full CFRP wrapping system.

4. Analytical modeling

An analytical model that accounts for the additional eccentricity caused by the lateral mid-height displacement and the confinement effect of CFRP under eccentric loading was employed to verify test results. The materials constitutive laws, basic assumptions and main components of the model are presented in details in Ref. [14]. In the model, the enhancement in strength and ultimate strain of concrete caused by CFRP wrapping is conservatively assumed to reduce as e/h is increased as follows:

$$f'_{cc} = f'_c + (f'_{cco} - f'_c)\left(\frac{1}{1+e/h}\right), \quad (1)$$

$$\varepsilon_{cc} = \varepsilon_{cu} + (\varepsilon_{ccu} - \varepsilon_{cu})\left(\frac{1}{1+e/h}\right), \quad (2)$$

where f'_{cc} and ε_{cc} are the strength and ultimate compressive strain of a CFRP-confined concrete at a given e/h value, f'_{cco} and ε_{ccu} are the strength and ultimate compressive strain of a CFRP-confined concrete under concentric loading, and ε_{cu} is the ultimate compressive strain of an unconfined concrete.

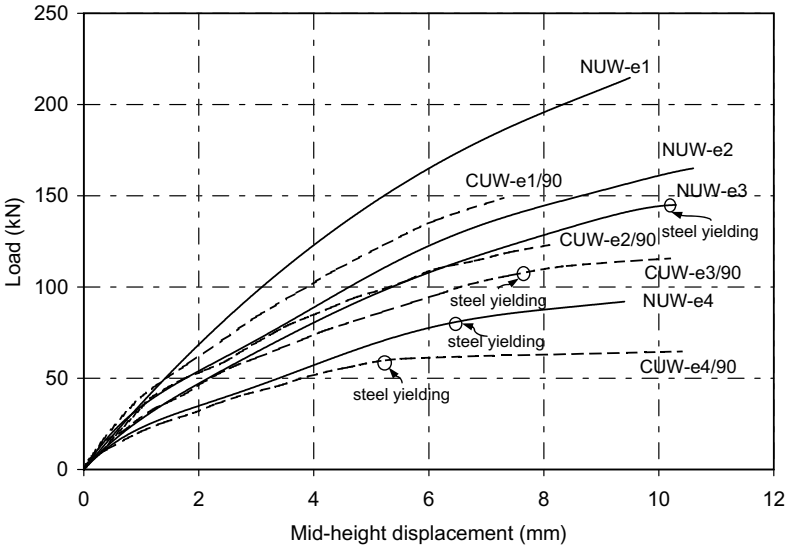

Fig. 8. Load versus mid-height displacement curves for groups [A] and [E].

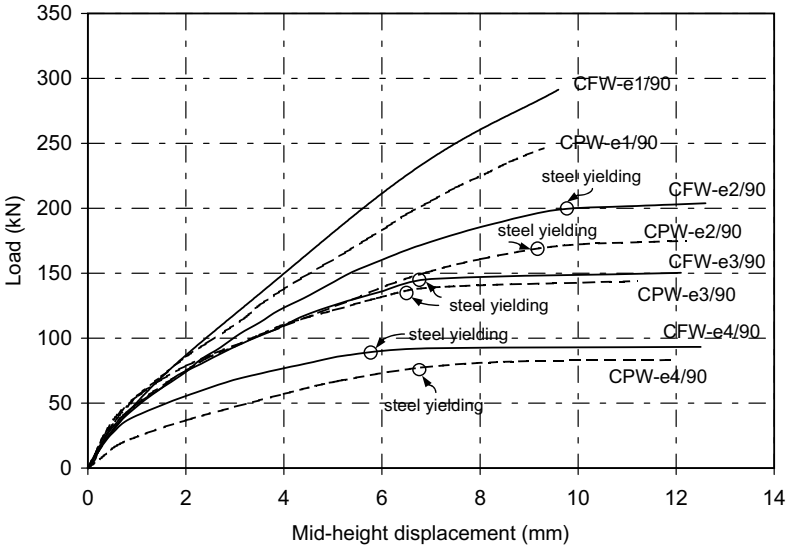

Fig. 9. Load versus mid-height displacement curves for groups [F] and [G].

The modeling procedure can be summarized as follows: step 1 – for a given initial eccentricity use the undeformed geometry to determine the sectional forces and curvature at the mid-height of the column; step 2 – use the mid-height sectional curvature to calculate the lateral mid-height displacement; step 3 – modify the initial eccentricity to account for the lateral mid-height displacement; step 4 – use the modified eccentricity to recalculate the sectional forces and curvature at the column's mid-height; step 5 – return to step 2 if there is a significant change in the sectional forces. A computer program was developed to carry out the modeling procedure. Flow chart of the program is given in Fig. 11. Methodologies for prediction of the confined concrete strength and ultimate strain under concentric loading, sectional forces, curvature and lateral displacement at the mid-height of the column are presented in Ref. [14].

Sectional geometry, material properties, and measured steel mass loss reported earlier were used as input data in the computer program. For the unwrapped specimens having 13.8% steel mass loss (group [E]), the clear concrete cover was neglected to account for the severe damage occurred in the concrete section. From Table 2, it can be seen that the predicted and measured deflections are in good agreement. The variation between the predicted and measured deflections had a negligible effect on the predicted strengths. All predicted strengths but that of specimen CUW-e3/90 were within 16% error band. The error in strength prediction for specimen CUW-e3/90 was −22% which can be ascribed to a variation between the actual steel mass loss and that measured from the corroded steel samples. It can then be concluded that the analytical model employed in this study gives reasonable predictions for the deflection and strength of

Table 2
Experimental and analytical results

Group	Specimen	Deflection capacity (mm)		Compression strength (kN)		Strength error (%)[a]
		Experimental (Δ_{exp})	Analytical (Δ_{pre})	Experimental (P_{exp})	Analytical (P_{pre})	
[A]	NUW-e1	9.5	6.7	215	212	−1
	NUW-e2	10.6	7.5	165	164	−1
	NUW-e3	10.3	8.2	145	132	−9
	NUW-e4	9.4	10.5	92	81	−12
[B]	CUW-e1/30[b]	NA	6.7	NA	208	NA
	CUW-e2/30	8.9	7.5	167	160	−4
	CUW-e3/30	9.3	8.2	141	129	−9
	CUW-e4/30	8.4	10.8	91	78	−14
[C]	CFW-e1/30	10.3	8.4	300	269	−10
	CFW-e2/30	10.0	9.5	208	207	−0.5
	CFW-e3/30	11.8	12.3	156	145	−7
	CFW-e4/30	10.6	15.5	97	83	−14
[D]	CPW-e1/30	9.9	7.5	276	264	−4
	CPW-e2/30	9.4	8.6	203	204	+0.5
	CPW-e3/30	11.5	10.5	153	146	−5
	CPW-e4/30	9.4	13.7	94	84	−11
[E]	CUW-e1/90	7.3	8.1	149	136	−9
	CUW-e2/90	8.2	9.0	124	109	−12
	CUW-e3/90	10.2	9.8	116	90	−22
	CUW-e4/90	10.4	14.6	65	58	−11
[F]	CFW-e1/90	9.6	8.5	290	262	−10
	CFW-e2/90	12.6	10.0	204	198	−3
	CFW-e3/90	12.1	12.8	150	136	−9
	CFW-e4/90	12.5	16	93	78	−16
[G]	CPW-e1/90	9.3	7.6	246	255	+4
	CPW-e2/90	12.2	8.7	175	196	+12
	CPW-e3/90	11.2	11.2	144	135	−6
	CPW-e4/90	12.0	14.5	83	77	−7

[a] Error (%) = $100 \times (P_{pre} - P_{exp})/(P_{exp})$.
[b] Specimen was broken during handling.

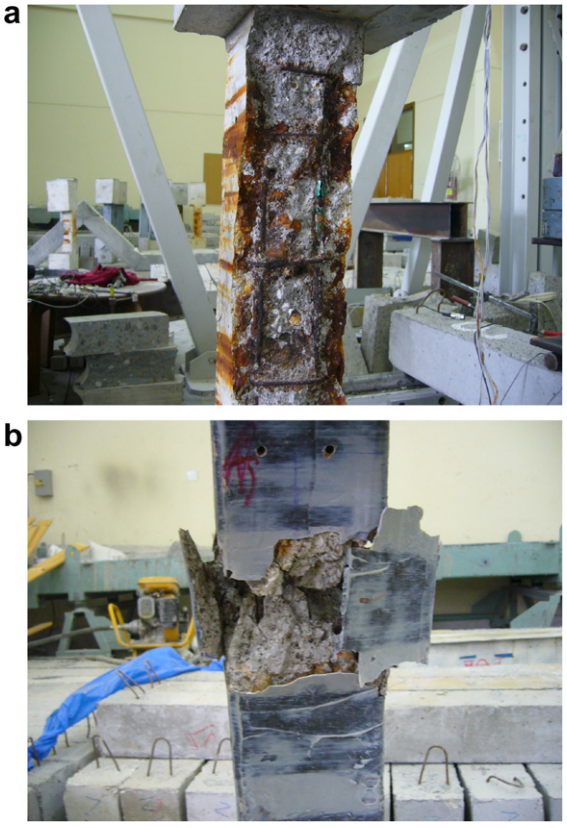

Fig. 10. Failure modes at the end of the post-repair stage: (a) corroded unrepaired specimens and (b) CFRP wrapped specimens.

both CFRP wrapped and unwrapped eccentrically loaded RC columns suffering from active corrosion.

5. Conclusions

The post-repair performance of corrosion-damaged eccentrically loaded RC columns wrapped with CFRP was examined in this paper. The main conclusions are as follows:

- For the unwrapped columns, 13.8% corrosion that corresponded to a maximum corrosion crack width of about 1.65 ± 0.35 mm significantly reduced the columns' strength. The strength reduction caused by 13.8% corrosion was in the range of 20–31%. About 23% reduction in deflection capacity was recorded at 13.8% corrosion when a compression mode of failure was dominated. The deflection capacity slightly increased at 13.8% corrosion when a tension mode of failure was dominated.
- During the post-repair corrosion phase, full CFRP wrapping system, with an effective confinement ratio of $f_l/f'_c = 0.2$, reduced the measured current by about 25% and 12% at fixed applied potentials of 12 and 15 V, respectively, relative the current of the unwrapped specimens. Partial CFRP wrapping with $f_l/f'_c = 0.12$ resulted in only 12% current reduction at applied fixed potential of 12 V whereas it had no noticeable effect on the measured current at a fixed applied potential of 15 V.
- At the end of the post-repair stage, the steel mass loss measured in the fully wrapped specimens ($f_l/f'_c = 0.2$) was about 28% lower than that of the unwrapped specimens. On the contrary, partial CFRP wrapping system ($f_l/f'_c = 0.12$) had almost no effect on the measured steel mass loss compared with that of the unwrapped specimens.

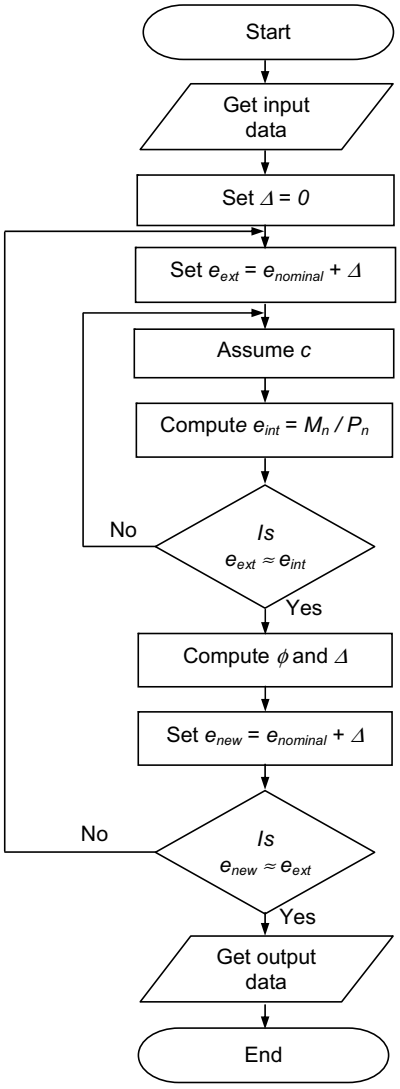

Fig. 11. Flow chart of the computer program.

- At the end of the post-repair corrosion exposure, the strengths of the specimens fully wrapped with CFRP ($f_l/f'_c = 0.2$) were still 35%, 24%, 3%, and 1% higher than those of the control undamaged specimens at nominal e/h values of 0.3, 0.43, 0.57, and 0.86, respectively. The strengths of the damaged specimens partially wrapped with CFRP ($f_l/f'_c = 0.12$) were 14% and 6% higher than those of the control specimens at nominal e/h values of 0.3 and 0.43, respectively. At higher e/h values the strength of the partially wrapped columns was lower than that of the control but still higher than that of the damaged unrepaired specimens.
- At the end of the second phase of corrosion exposure, the deflection capacity of the specimens fully wrapped with CFRP ($f_l/f'_c = 0.2$) at e/h values of 0.3 and 0.43 was on average 43% higher than that of their counterparts that were corroded but unwrapped with CFRP. Only 20% average increase in deflection capacity due to full CFRP wrapping was recorded at e/h values of 0.57 and 0.86. The deflection capacities of the columns partially wrapped with CFRP ($f_l/f'_c = 0.12$) were almost the same as those of their counterparts repaired with full CFRP wrapping system.

Acknowledgements

The author would like to express his appreciation to the Research Affairs at the UAE-University for the financial support of this project under fund grant # 03-01-7-11/07. The author would like to express his gratitude to the undergraduate research assistants and the laboratory specialists at the UAE-University for their help throughout testing.

References

[1] Tuutti K. Service life of structures with regard to corrosion of embedded steel. Performance of concrete in marine environment. ACI SP-65. Detroit (MI): American Concrete Institute; 1980. p. 223–36.
[2] Weyers RE. Service life model for concrete structures in chloride laden environments. ACI Mater J 1998;95(4):445–53.
[3] El Maaddawy TA, Soudki KA. A model for prediction of time from corrosion initiation to corrosion cracking. Cement Concr Compos 2007;29(3):168–75.
[4] Bonacci JF, Maalej M. Externally bonded fiber-reinforced polymer for rehabilitation of corrosion damaged concrete beams. ACI Struct J 2000;97(5):703–11.
[5] El Maaddawy TA, Soudki KA. Carbon-fiber-reinforced polymer repair to extend service life of corroded reinforced concrete beams. ASCE J Compos Constr 2005;9(2):187–94.
[6] El Maaddawy TA, Soudki KA, Topper T. Performance evaluation of carbon fiber reinforced polymer-repaired beams under corrosive environmental conditions. ACI Struct J 2007;104(1):3–11.
[7] Lee C, Bonacci J, Thomas M, Maalej M, Khajehpour S, Hearn N, et al. Accelerated corrosion and repair of reinforced concrete columns using fibre reinforced polymer sheets. Can J Civil Eng 2000;27(5):941–8.
[8] Pantazopoulou S, Bonacci J, Sheikh S, Thomas M, Hearn N. Repair of corrosion-damaged columns with FRP wraps. ASCE J Compos Constr 2001;5(1):3–11.
[9] Debaiky A, Green M, Hope B. Carbon fiber-reinforced polymer wraps for corrosion control and rehabilitation of reinforced concrete columns. ACI Mater J 2002;99(2):129–37.
[10] Parvin A, Wang W. Behavior of FRP jacketed concrete columns under eccentric loading. ASCE J Compos Constr 2001;5(3):146–52.
[11] Chaallal O, Shahawy M. Performance of fiber-reinforced polymer-wrapped reinforced concrete column under combined axial–flexural loading. ACI Struct J 2000;97(4):659–69.
[12] Hadi M. Behaviour of FRP wrapped normal strength concrete columns under eccentric loading. J Compos Struct 2006;74:503–11.
[13] El Maaddawy TA. Behavior of corrosion-damaged RC columns wrapped with FRP under combined flexural and axial loading. Cement Concr Compos 2008;30(6):524–34.
[14] El Maaddawy TA. Strengthening of eccentrically loaded reinforced concrete columns with fiber-reinforced polymer wrapping system. ASCE J Compos Constr; in press.
[15] ASTM International. Standard practice for preparing, cleaning, and evaluating corrosion test specimens. ASTM G1-90; 2002.